ChemComm

Accepted Manuscript

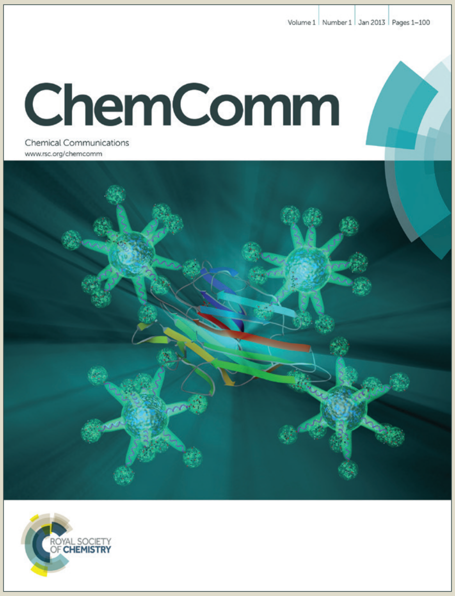

ROYAL SOCIETY OF CHEMISTRY

www.rsc.org/chemcomm

Cite this: DOI: 10.1039/c0xx00000x

www.rsc.org/ chemcomm

COMMUNICATION

Template-Free Synthesis of Beta Zeolite Membranes on Porous α-Al_2O_3 Supports

Yanting Tang, Xiufeng Liu, Shifeng Nai & Baoquan Zhang *

Received (in XXX, XXX) Xth XXXXXXXXX 201X, Accepted Xth XXXXXXXXX 201X

DOI: 10.1039/b000000x

The preferentially (*h0l*)-oriented beta zeolite membrane was prepared on the porous α-Al_2O_3 support by secondary growth of a beta seed layer in the absence of organic templates.

The first practical application of zeolite membranes appeared in 1997[1]. Despite intense research afterwards, zeolite membranes fall short of gaining commercial applications worldwide because of their unsatisfactory performances, high costs, and difficulties in scaling up[2]. An ideal zeolite membrane should be free from pinholes and cracks with highly cross-linked zeolite crystals being fully covered on the support. However, the existence of defects in polycrystalline zeolite membranes cannot be avoided if they are prepared using organic templates. As for a zeolite membrane prepared in the presence of organic templates, the template removal must be done before it is applied in practical usage. Typically, the removal of organic templates from zeolite membranes occurs at 450~550 ℃, leading to the shrinkage in the framwork of zeolite crystals. Due to the difference in thermal expansion between the zeolite top-layer and the porous support, the intercrystal boundary gaps and micro-cracks would be formed during the template removal at high temperatures[3]. Although the cracks could be repaired by the post-synthetic treatment[4], the organic template-free method averts the use of expensive organic templates and the formation of defects in the following template-removal step.

Currently, FAU-, MOR-, MFI-, FER-, LTA- and BEA-type zeolites have reached industrial use and cover more than 90% of all the applications[5]. Zeolite beta (BEA) possesses a three-dimensional 12-membered ring pore structure consisting of 6.6 × 6.7 Å channels running straight along the *a* (or *b*) axis and 5.6 × 5.6 Å channels running tortuously along the *c* axis[6,7]. Beta zeolite membranes could be synthesized via in situ crystallization or secondary growth method using organic agents as templates. At present, it still needs to consume a substantial amount of organic templates for the synthesis of beta zeolite membranes. Comparing with the synthesis of MFI type zeolite membranes ($H_2O/(TPA)_2O$ = 95~∞[8–13]), the consumption of organic templates for the synthesis of beta zeolite membranes is much greater ($H_2O/(TEA)_2O$ = 20~172)[7,14–19]. Tetraethylammonium hydroxide (TEAOH) usually used as the organic template for preparing beta zeolite membranes, is always the most costly part. Thus, the template-free method reduces the cost of synthesizing beta zeolite membranes remarkably, which would be more possible to gain wide commercial applications. Historically, the template-free secondary growth method has been applied to prepare MFI and CHA-type zeolite membranes[11,12,20]. However, it is still unsuccessful to synthesize a beta zeolite membrane without organic templates yet. Fortunately, the seed-induced, organic template-free synthesis of zeolite beta has been developed since 2008[21], which offers a possibility to prepare beta zeolite membranes in the absence of organic templates.

In the present work, we report an organic template-free synthesis strategy to prepare a preferentially (*h0l*)-oriented beta zeolite membrane on the porous α-Al_2O_3 support surface by secondary growth method. To our best knowledge, this is the first report of the organic template-free synthesis strategy for beta zeolite membranes. Notably, the template-free method averts the formation of calcination defects because as-synthesized beta zeolite membranes already own open micropores. Moreover, it not only avoids the environmental pollution, but also reduces the cost significantly.

As a typical run, the beta zeolite membrane was prepared on the porous α-Al_2O_3 support by template-free secondary growth method in the precursor suspension with the molar composition of 30 SiO_2: Al_2O_3: 10 Na_2O: 900 H_2O at a temperature of 140 ℃ for 5 d. Fig. S1 (ESI†) shows the scanning electron microscope (SEM) image, X-ray diffraction (XRD) pattern, thermogravimetric (TG) analyses of zeolite beta, and Fourier transform infrared spectoscopy (FT-IR) spectra of zeolite beta before and after calcination. The average size of beta crystals is 268 nm (determined by Malvern Zetasizer).

The surface of the beta seed layer was flat with a thickness of ca. 1.5 μm after spin coating (Fig. 1a, and 1b). The morphology and structure of the beta zeolite membranes were characterized with SEM and XRD. As shown in Fig. 1c-1f, after template-free hydrothermal synthesis, the surface of the α-Al_2O_3 disk was covered by plenty of crystals, which formed a dense zeolite film with a thickness of ca. 3 μm on the support. Some beta crystals smaller than the pore size of the α-Al_2O_3 support (ca. 0.2 μm)[22] fell into the pores of the support and grew up, which made the boundary between the beta zeolite membrane and the α-Al_2O_3 support fuzzy. The zeolite film is composed of well intergrown crystals. As revealed in XRD patterns (Fig. 2), the membrane only exhibited the typical peaks of BEA structure and α-Al_2O_3, which indicated that the pure beta film was successfully prepared from the organic template-free synthesis suspension. The XRD pattern of the beta-OTF (beta organic template-free) zeolite membrane displayed diffraction peaks at 2θ = 7.64, 22.10, 25.02, 28.34, 29.2 ° corresponding to the reflections that arise from (101), (302), (304), (401), and (306) planes (Fig. S2 in ESI† demonstrated all the lattice planes), confirming all the beta crystals on the film surface are preferentially (*h0l*)-oriented, which could also be described as *c*-out-of-plane orientation[23].

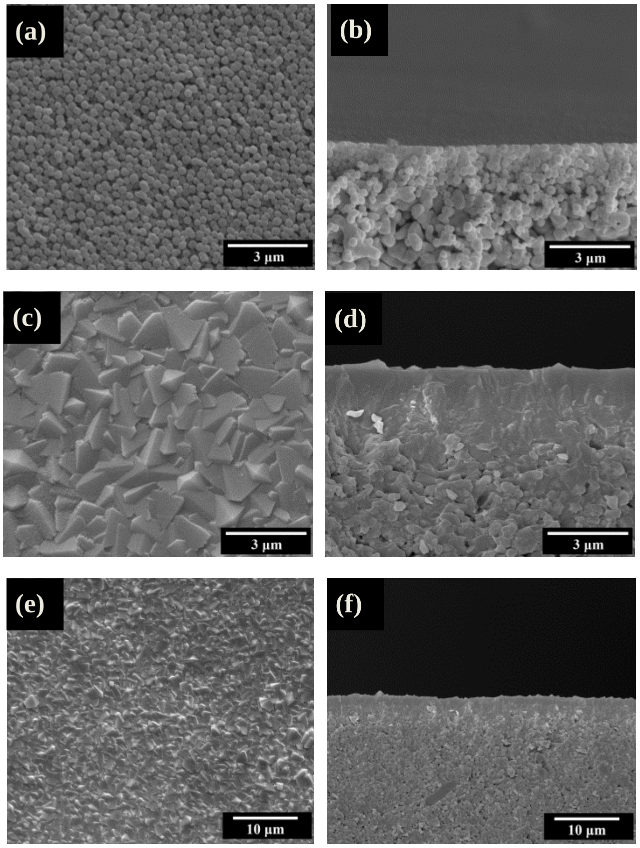

Fig. 1. Top view (a) and cross-section view (b) SEM images of the beta seed layer on α-Al_2O_3 support; top view (c, and e) and cross-section view (d, and f) SEM images of the beta-OTF zeolite membrane on α-Al_2O_3 support at different magnifications.

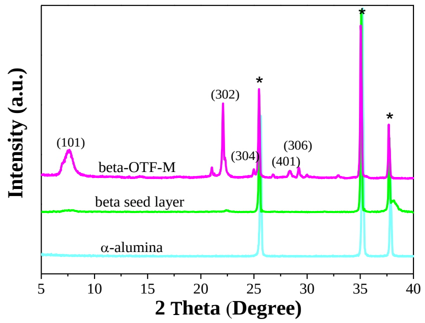

Fig. 2. XRD patterns of the α-Al_2O_3 support, the seed layer, and the beta-OTF zeolite membrane (beta-OTF-M).

In the template-free secondary growth route, Na^+ cation replaces the TEA^+ cation to balance the negative charge of beta zeolite framework. The energy dispersive x-ray analysis (EDAX) of the as-synthesized membrane revealed that the Si/Na ratio was 48.8. It makes beta zeolite membranes more stable, as the TEA^+ cation must be removed after synthesis. The morphology of as-synthesized beta zeolite membranes revealed some differences with the membranes prepared from the same condition except for using uncalcined seed layer (Fig. S3a, ESI†) . Meanwhile, the thickness of the latter one was ca. 4 µm (Fig. S3b, ESI†), and the product collected from the bottom of autoclave was amorphous (Fig. S4a and S5a, ESI†). It is implied that more of beta crystals in the seed layer dropped to the bottom of the autoclave after calcination, which played a role as seeds to induce the formation of intergrown zeolite beta possessing a truncated octahedral morphology in the template-free suspension after hydrothermal synthesis (Fig. S4b, ESI†). However, it didn't affect the continuity of the film. Zeolite beta is only part of the product, and most of the powder product was amorphous (Fig. S5b, ESI†).

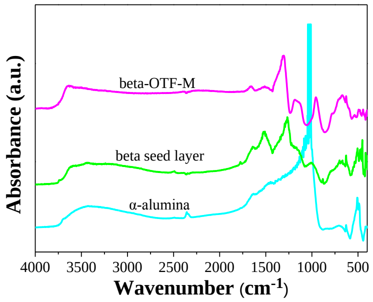

Fig. 3. FT-IR spectra of the α-Al_2O_3 support, the seed layer, and the beta-OTF zeolite membrane.

The FT-IR spectra of the zeolite beta before and after calcination are presented in Fig. S1d (ESI†). The bands at 2987, 1485 and 1394 cm^{-1} are attributed to TEAOH, which disappeared after calcination. Fig. 3 shows the FT-IR spectra of α-Al_2O_3 support, the seed layer, and the beta-OTF zeolite membrane. The bands of the beta-OTF zeolite membrane corresponding to the calcined zeolite beta. For the beta-OTF zeolite membrane, the intensity of the characteristic peaks of the α-Al_2O_3 support at 1024 and 490 cm^{-1} decreased or disappeared, and the framework absorption peaks of zeolite beta at 1182 and 958 cm^{-1} increased comparing with the beta seed layer[24]. This is consistent with the results of XRD.

Without organic templates, appropriate molar ratios of the precursor suspension and hydrothermal synthesis condition were crucial to prepare a continuous and compact beta zeolite membrane. Besides, the placement of the support also influenced the synthesis of the beta zeolite membranes greatly. The beta-OTF zeolite membranes were synthesized in the condition of the seeded α-Al_2O_3 support placed horizontal downwards. When the support was placed horizontal upwards, the surface of the membrane was covered with a lot of gel and undesired species (Fig. S6, ESI†). It is suggested that the placement of horizontal downwards is conducive to the growth of the beta seeds on the α-Al_2O_3 support, making it much more easily to obtain pure beta zeolite membranes. It is reported that the addition of beta seeds is indispensable for the synthesis of zeolite beta in the aluminosilicate gel or suspensions without any organic templates. Beta seeds must be present in the organic template-free synthesis route of zeolite beta[21]. Similarly, the beta seed layer is also necessary for the synthesis of beta zeolite membranes in the organic template-free precursor suspensions. Without that, only a gel layer could be obtained in the same hydrothermal synthesis condition (Fig. S7, ESI†), which generated cracks easily after dried in the oven.

When zeolite membranes are prepared with organic templates, the quality could be detected by the light gas. A perfect zeolite membrane exhibited gas tightness before the removal of organic templates. However, the means is not suitable for the template-free zeolite membranes, because as-synthesized beta zeolite membranes already own open micropores. Therefore, the permeation of larger molecules by pervaporation may be a much better indication of membrane quality, especially for medium and large-pore template-free zeolite membranes. 1,3,5-triisopropylbenzene (TIPB) is an appropriate candidate, since its kinetic diameter (0.85 nm) is larger than the pore size of zeolite beta. In order to evaluate the quality of the most promising beta zeolite membranes, pervaporation experiments were carried out at 303 K with pure components including water, methanol, ethanol, n-butanol, methyl tertiary butyl ether (MTBE), and TIPB. The results are given in Fig. 4 and Table 1.

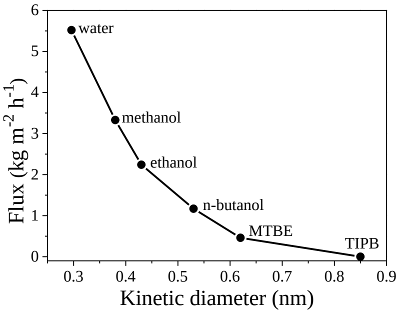

Fig. 4. Pervaporation fluxes of pure components at 303 K as a function of kinetic diameter for the beta-OTF zeolite membrane.

Table 1 Summary of pervaporation performance for pure TIPB component, and separation of TIPB/ethanol mixture achieved in this work and by other groups.

T (°C)	TIPB (wt %)	Total Flux (kg m^{-2} h^{-1})	TIPB Flux (kg m^{-2} h^{-1})	$\alpha_{E/T}$	Ref.
30	10	1.5798	0.00055	321	This work
30	100	~0	~0	/	This work
30	100	0.0053	0.0053	/	[14, 15]
25	100	0.001	0.001	/	[17]
25	10	/	/	32	[18]

There is almost no TIPB detected in the permeate side of the beta zeolite membrane. The fluxes and separation factors estimated by Eqs. (1) and (2) (pervaporation test, ESI†), respectively, are presented as an average of the three values measured during the 4 hr pervaporation experiment. These results suggested that beta-OTF zeolite membranes are better than the ones synthesized by the template-method. The most selective membrane exhibited an ethanol/TIPB separation factor of 321 for a mixture containing 10 wt % TIPB diluted in ethanol. The fraction of permeate TIPB was only 0.03 wt %, and the total flux was 1.58 kg m^{-2} h^{-1}. It was concluded that little pinholes and cracks existed in the membrane.

In conclusion, an organic template-free route for synthesizing beta zeolite membranes by secondary growth method is provided. Under appropriate molar ratios of the precursor suspension and hydrothermal conditions, the calcination of the seed layer and the placement of the support influenced the synthesis of beta zeolite membranes greatly without organic templates. Most importantly of all, the beta seed layer is indispensable for the template-free route. It is noteworthy that the template-free route could avoid the consumption of organic templates, the formation of calcination defects and the pollution to the environment, which would be very helpful for green and cheap synthesis of beta zeolite membranes, as well as more possible to realize wide commercial applications.

This work was supported by the National Natural Science Foundation of China (21076154 and 21136008), and the State Oceanic Administration of China (201105026).

Notes and references

State Key Laboratory of Chemical Engineering, School of Chemical Engineering and Technology, Tianjin University, Tianjin 300072, China
Tel: 86 22 27408785 E-mail*: bqzhang@tju.edu.cn*

† Electronic Supplementary Information (ESI) available: Experimental and supporting data. See DOI: 10.1039/b000000x/

1. M. Kondo, M. Komori, H. Kita and K. Okamoto, *J. Membr. Sci.*, 1997, **133**, 133–141.
2. J. Caro and M. Noack, *Microporous Mesoporous Mater.*, 2008, **115**, 215–233.
3. J. H. Dong, Y. S. Lin, M. Z. C. Hu, R. A. Peascoe and E. A. Payzant, *Microporous Mesoporous Mater.*, 2000, **34**, 241–253.
4. B. Q. Zhang, C. Wang, L. Lang, R. L. Cui and X. F. Liu, *Adv. Funct. Mater.*, 2008, **18**, 3434–3443.
5. V. Valtchev, G. Majano, S. Mintova and J. Pérez-Ramírez, *Chem.* Soc. Rev., 2013, 42, 263–290.
6. Database of Zeolite Structures, http://www.iza-structure.org/databases/, International Zeolite Association (accessed Mar. 12, 2014)
7. C. T. P. Tung, H. S. Kim and K. B. Yoon, *Science*, 2011, **334**, 1533–1538.
8. Z. A. E. P. Vroon, K. Keizer, A. J. Burggraaf and H. Verweij, *J. Membr. Sci.*, 1998, **144**, 65–76.
9. Z. Wang and Y. Yan, *Chem. Mater.*, 2001, **13**, 1101–1107.
10. L. Lang, X. F. Liu, H. Y. Jiang, J. Y. S. Lin and B. Q. Zhang, *Langmuir*, 2010, **26**, 5895–5900.
11. S. Mintova, J. Hedlund, V. Valtchev, B. J. Schoeman and J. Sterte, *J. Mater. Chem.*, 1997, **7**, 2341–2342.
12. W. H. Yuan, Y. S. Lin and W. S. Yang, *J. Am. Chem. Soc.*, 2004, **126**, 4776–4777.
13. L. Lang, X. F. Liu, M. L. Hu and B. Q. Zhang, *ChemCatChem*, 2009, **1**, 472–478.
14. V. A. Tuan, S. G. Li, J. L. Falconer and R. D. Noble, *Chem. Mater.*, 2002, **14**, 489–492.
15. V. A. Tuan, L. L. Weber, J. L. Falconer and R. D. Noble, *Ind. Eng. Chem. Res.*, 2003, **42**, 3019–3021.
16. A. Jakob, V. Valtchev, M. Soulard and D. Faye, *Langmuir*, 2009, **25**, 3549–3555.
17. Y. L. Chen, G. S. Zhu, Y. Peng, X. D. Yao and S. L. Qiu, *Microporous Mesoporous Mater.*, 2009, **124**, 8–14.
18. P. S. Barcia, A. Ferreira, J. Gascon, S. Aguado, J. A. C. Silva, A. E. Rodrigues and F. Kapteijn, *Microporous Mesoporous Mater.*, 2010, **128**, 194–202.
19. M. Navlani-García, F. J. Varela-Gandía, A. Bueno-López, D. Cazorla-Amorós, B. Puértolas, J. M. López, T. García and D. Lozano-Castelló, *ChemSusChem*, 2013, **6**, 1467–1477.
20. Y. Hasegawa, H. Hotta, K. Sato, T. Nagase and F. Mizukami, *J. Membr. Sci.*, 2010, **347**, 193–196.
21. B. Xie, J. W. Song, L. M. Ren, Y. Y. Ji, J. X. Li and F. S. Xiao, *Chem. Mater.*, 2008, **20**, 4533–4535.
22. X. D. Wang, B. Q. Zhang, X. F. Liu and J. Y. S. Lin, *Adv. Mater.*, 2006, **18**, 3261–3265.
23. Y. S. Li, H. Bux, A. Feldhoff, G. L. Li, W. S. Yang and J. Caro, *Adv. Mater.*, 2010, **22**, 3322–3326.
24. R. Kumar, A. Thangaraj, R. N. Bhat and P. Ratnasamy, *Zeolites*, 1990, **10**, 85–89.